Geomechanics and Engineering, *Vol. 24, No. 2 (2021) 157-166*
DOI: https://doi.org/10.12989/gae.2021.24.2.157

Mechanical behavior of Beishan granite samples with different slenderness ratios at high temperature

Qiang Zhang*[1], Yanjing Li[1a], Ming Min[2b] and Binsong Jiang[1c]

[1]*School of Mechanics and Civil Engineering, State Key Laboratory for Geomechanics and Deep Underground Engineering, China University of Mining and Technology, Xuzhou 221116, China*
[2]*School of Civil and Hydraulic Engineering, Huazhong University of Science and Technology, Wuhan 430074, China*

(Received December 7, 2019, Revised December 28, 2020, Accepted January 8, 2021)

Abstract. This paper aims at the temperature and slenderness ratio effects on physical and mechanical properties of Beishan granite. A series of uniaxial compression tests with various slenderness ratios and temperatures were carried out, and the acoustic emission signal was also collected. As the temperature increases, the fracture aperture of intercrystalline cracks gradually increases, and obvious transcrystalline cracks occurs when T > 600℃. The failure patterns change from tensile failure mode to ductile failure mode with the increasing temperature. The elastic modulus decreases with the temperature and increases with slenderness ratio, then tends to be a constant value when T = 1000℃. However, the peak strain has the opposite evolution as the elastic modulus under the effects of temperature and slenderness ratio. The uniaxial compression strength (UCS) changes a little for the low-temperature specimens of T < 400℃, but a significant decrease happens when T = 400℃ and 800℃ due to phase transitions of mineral. The evolution denotes that the critical brittle-ductile transition temperature increases with slenderness ratio, and the critical slenderness ratio corresponding to the characteristic mechanical behavior tends to be smaller with the increasing temperature. Additionally, the AE quantity also increases with temperature in an exponential function.

Keywords: rock; mechanical behavior; acoustic emission; high temperature; slenderness ratio

1. Introduction

The mechanical and acoustic emission (AE) characteristics of rock mass are the foundation for the stability evaluation in rock engineering. In many special projects, such as nuclear waste repository, geothermal energy utilization, underground coal gasification and underground storage, the rock mass may be affected by high temperature. High temperature causes the expansion, chemical reactions and thermal damage in rock material (Sun *et al.* 2015), which results in a significant change in mechanical properties of rocklike materials (Su *et al.* 2020). These changes may cause irreparable loss if they are not reasonably considered in the engineering stability evaluation.

In the last decades, a lot of achievements were made on the mechanical behavior of rock under high temperature treatment, mainly considering uniaxial compression stress (UCS), elastic modulus, strain, fracture toughness and AE characteristics (Dwivedia *et al.* 2008, Ranjith *et al.* 2012, Brotóns *et al.* 2013, Kong *et al.* 2016, Peng *et al.* 2016, Tian *et al.* 2017, Yin *et al.* 2012a, b, Heuze 1983, Lau *et al.* 1995, Guo *et al.* 2020). Chen *et al.* (2012) investigated the evolution of peak stress, peak strain and elastic modulus subjected to thermal treatment granite from 20 to 1000ºC. The results denote that the peak stress and elastic modulus decreases with the increasing heat treatment temperature, while the peak strain decreases as the heat treatment temperature. Xu *et al.* (2008) also investigated the thermal effect of granite ranging from 20 to 1200ºC, finding that there was an obvious variation occurred in granite when the temperature was lower than 800ºC; its strength significantly dropped above 800ºC, and the bearing capacity almost lost at 1200ºC. Liang *et al.* (2012) studied the deformation and failure mode of large size granite at high temperatures and pressures, obtaining the dynamic elastic modulus for various temperatures. Liu *et al.* (2015) investigated both the physical and mechanical properties of granite and sandstone samples after high-temperature treatment, indicating that the rock density generally decreases with the increase in temperature and 600°C (800°C) were the critical temperatures corresponding to the brittle-ductile for granite (sandstone). Zhang *et al.* (2014) investigated the variation of the peak strain, peak stress and elastic modulus of mudstone at high temperature according to the uniaxial compression tests. Clearly, most of the thermal effect experiments were carried out with respect to the heat treatment rock mass due to the difficulty of experimental equipment. The AE characteristic of rock is important to the rockburst and failure process monitoring of engineering in complex geological environment (Zhang *et al.* 2017,

*Corresponding author, Ph.D.
E-mail: jakezhq@126.com
[a]M.D. Student
E-mail: yjl@cumt.edu.cn
[b]M.D. Student
E-mail: minming@cumt.edu.cn
[c]Ph.D.
E-mail: jiangbs@cumt.edu.cn

ISSN: 2005-307X (Print), 2092-6219 (Online)

Ercikdi *et al.* 2016). Jamshidi *et al.* (2018) proposed a prediction method of uniaxial compressive strength with density and P-wave velocity. Wu *et al.* (2018) analyzed the strength, deformation, acoustic emission (AE) and failure characteristics of cracked rock specimen. Ercikdi *et al.* (2016) studied the effect of the core length on the saturated and dry P-wave velocities of four different biomicritic limestone samples using core samples having different lengths (25-125 mm) at a constant diameter (54.7 mm). The results denote that the P-wave velocities of limestone samples increased or decreased with increasing samples size, and the dry samples produced consistently 1.03-1.46 times higher than those of saturated samples at higher sample lengths (75, 100 and 125 mm).

At the earliest, size effects on rock strength were carried out by Bieniawski (1967) and Pratt *et al.* (1971). Later, Hoek and Brown (1980) proposed the well-known empirical size-effect model by collecting numbers of published papers on size-effect data. Since the International Workshops on Scale Effects in Rock Masses (held in Loen, Norway in 1990), a basic understanding of scale effects in rock mechanics was established, and lots of studies concluded that the size effects mainly depended on rock type, texture, micro-flaws, loading conditions and so on according to the uniaxial compression tests (Hawkins 1998, Yoshinaka *et al.* 2008, Pierce *et al.* 2009). However, Masoumi *et al.* (2016) pointed out that the strength of significant small specimens monotonically decreased with the increase of size, which was different from the widely accepted evolutional laws. Ding *et al.* (2013) numerically analyzed the mechanical behavior of size-effect by PFC3D procedure with the modified specimen generation method. The simulated results denoted that, with a larger diameter to median particle size ratios, the simulated UCS still increases, but the rate is much smaller; the average simulated Young's modulus decreases; and the average simulated Poisson's ratio remains approximately the same.

Obviously, a lot of achievements on the thermal and size-effect have been made in the past decades. But most of the studies about thermal effects were carried out with respect to the thermal treatment specimens under the indoor temperature because of limitations due to experimental conditions to keep the high temperature during the loading process. But the mechanical properties of rock mass at indoor temperature are obviously different from those at high temperature (Yin *et al.* 2016). For high-temperature engineering, the temperature may also influence the size-effect. Unfortunately, few experimental studies on the mechanical and AE characteristics considering both the high temperature and size-effect, which is important for the stability analysis. To provide reasonable mechanical properties of rock mass in large-scale high temperature engineering, the mechanical behavior of granite with various slenderness ratio at high temperature is studied according to the uniaxial compression tests.

2. Experimental tests

2.1 Sample preparation

The granite block samples were retrieved from the Beishan district, Gansu, China, where the high-level radioactive waste repository laboratory was preselected. According to the size of high-temperature furnace and the standard requirements of the International Society of Rock Mechanics with the parallelism controlled within ±0.05 mm and surface flatness within ±0.02 mm, cylindrical specimens of diameter of 25 mm with slenderness ratio *L/D* = 1.0, 2.0, 3.0 and 4.0 for uniaxial compression tests were prepared, and samples with similar longitudinal wave velocity tested by RSM-SY6 were selected.

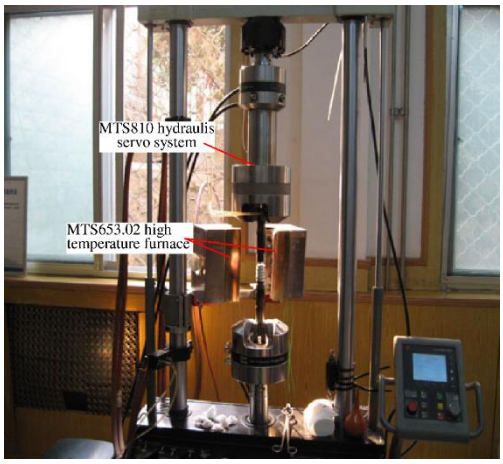

Fig. 1 The MTS810 hydraulic servo system and MTS653.02 high-temperature furnace

2.2 Experimental equipment

The uniaxial compression tests were carried out with the electro-hydraulic servo-controlled material testing machine MTS810, and the samples were heated by the assorted high-temperature furnace MTS653.02 with a heated range of D58 × 220 cm, as shown in Fig. 1. Six temperature levels of 25ºC, 200ºC, 400ºC, 600ºC, 800ºC, and 1000ºC were selected. Before the axial loading, the rock sample was heated with a rate of 10ºC/min. After the environment temperature reached the preset value, the temperature was maintained for 30mins. Then, the uniaxial compression tests were carried out with a loading rate of 0.002 mm/s while the environmental temperature is maintained. During the compression tests process, the acoustic emission signal was detected and recorded with PCI2.

3. Results and discussion

The results of the experiment tests are discussed in the following four aspects: (1) deformation characters, (2) uniaxial compression strength, (3) microscopic and macroscopic observations, and (4) acoustic emission characters.

3.1 Deformation characteristics

The stress-strain curves with various slenderness ratio and temperature are shown in Fig. 2. When the temperature is lower than 800ºC, the stress-strain curve shows an

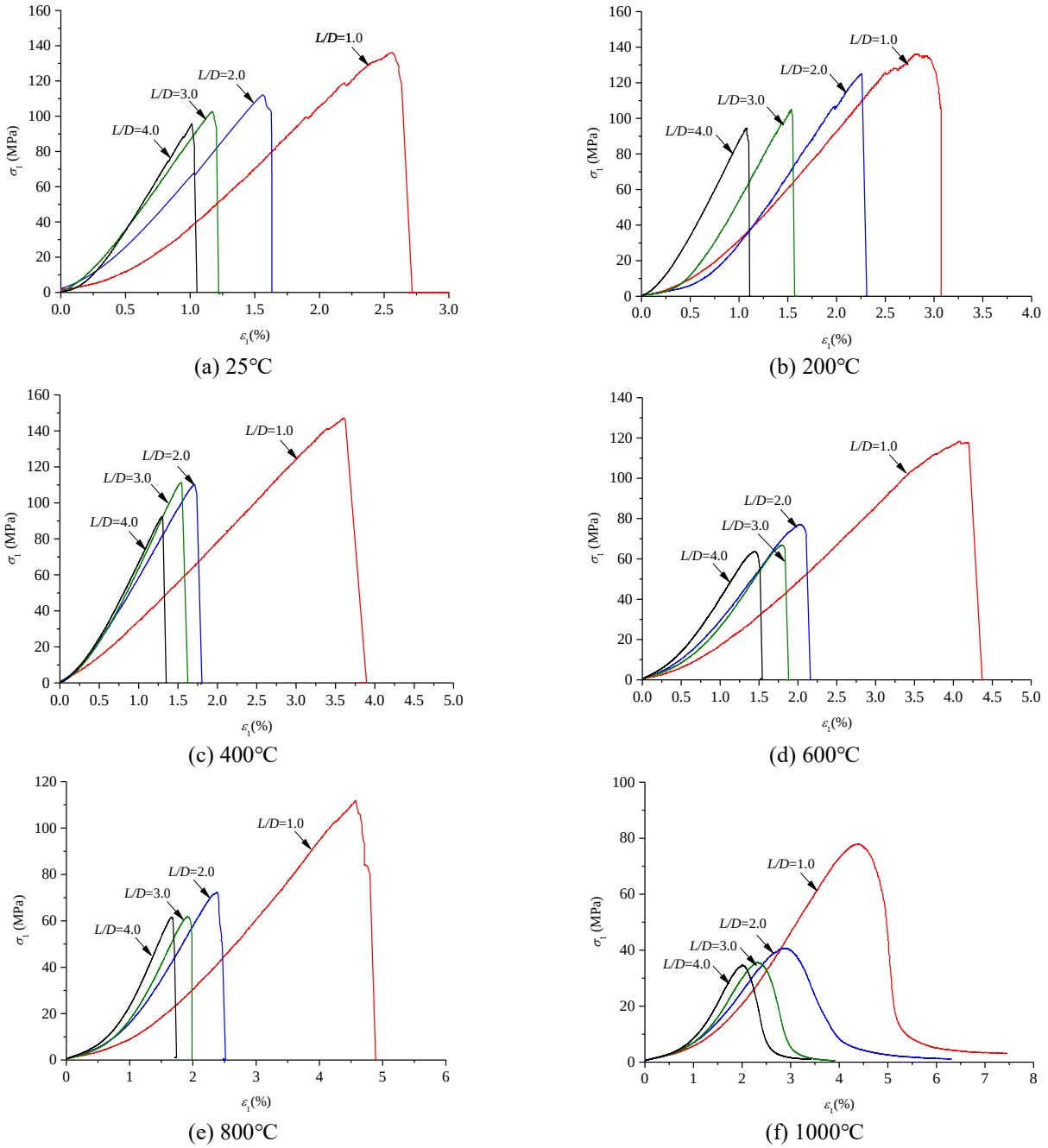

Fig. 2 Stress-strain curves with different temperatures and slenderness ratio

approximately linear relation until the peak strength is reached, then brittle failure occurs accompanying a sudden drop of uniaxial stress to zero. However, when the temperature reaches 1000ºC, the post-failure rock mass manifests a smooth progressive strain-softening failure process, and the residual strength tends to be zero when the axial strain is significant large. This is mainly induced by the granulation within a small region and is also in accordance with the microscopic and macroscopic observation results. For the specimens with the same temperature, the initial nonlinear section of specimens with small slenderness ratio is longer than those with large slenderness ratio due to the surface flatness issue. Take the specimens with L/D=4.0 as example, the axial strains at the starting point of elastic strain are about 0.2%, 0.25%, 0.3%, 0.37%, 0.9% and 1.1% corresponding to T= 25ºC, 200ºC, 400ºC, 600ºC, 800ºC and 1000ºC, respectively. In other words, the porosity of the high-temperature treated samples increases with the increasing temperature, and this is in accordance with the micro-observation. With the increase in slenderness ratios, the uniaxial strengh and peak strain decrease. Therefore, the mechanical properties of granite obviously depend on both of the temperature and slenderness ratios.

Fig. 3 shows the elastic modulus of granite with different slenderness ratio. With the increase in temperature, the elastic modulus gradually decreases for various slenderness ration specimens, and the decreasing ratio

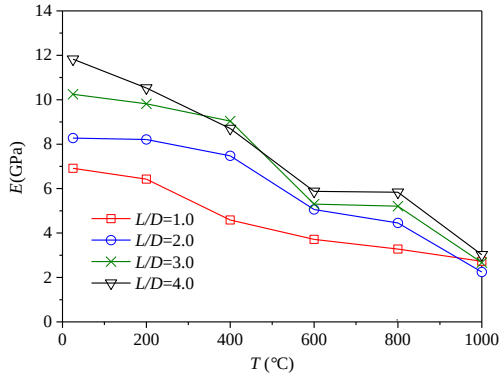

(a) Influence of temperature on elastic modulus

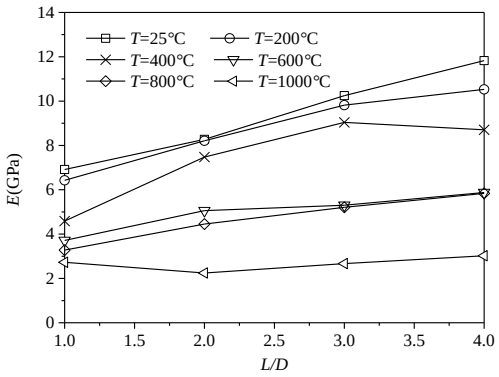

(b) Influence of slenderness ratio on elastic modulus

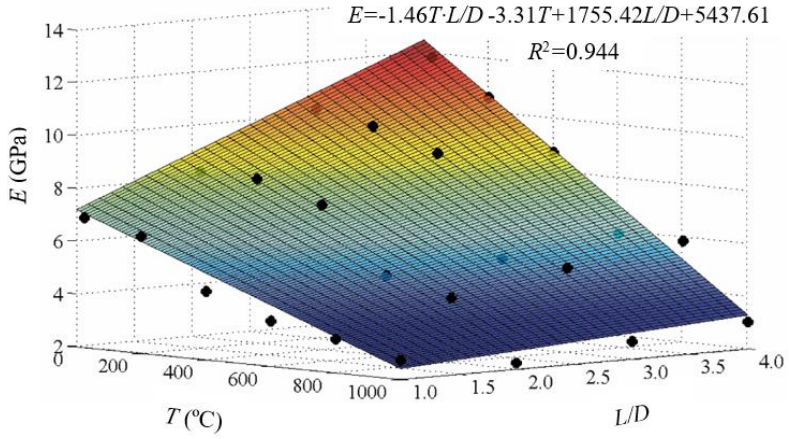

(c) Predicted elastic modulus by temperature and slenderness ratio

Fig. 3 Evolution of elastic modulus with different temperature and slenderness ratio

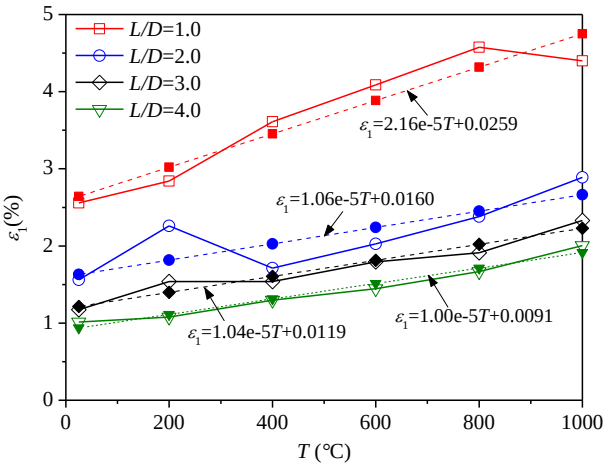

Fig. 4 Evolution of peak strain with different temperature and slenderness ratio

decrease of specimen with L/D = 4.0 is smaller than that of L/D = 1.0, i.e., the decreasing ratio of the two specimens are -8.86 GPa/ºC and -4.54 GPa/ºC. The elastic modulus approximately linearly increases with slenderness ratio, and the increasing ratio gradually decrease with the increase in temperature, i.e., an increasing ratio of 1.67 GPa and 0.13 GPa corresponding to T = 25ºC and 1000ºC, respectively. Thus, the slenderness ratio effect becomes inconspicuous for specimens under high temperature, and the elastic modulus tends to be a constant with an average value of 2.67 GPa at T = 1000ºC. The elastic modulus also decreases with the increase in temperature approximately in a linear way. Therefore, the elastic modulus increases with slenderness ratio and decreases with the temperature, and it can be expressed by a function of temperature and slenderness ratio as follows:

$$E = -\frac{1.46TL}{D} - 3.31T + \frac{1755.42L}{D} + 5437.61 \quad (1)$$

The evolution of peak strain with various slenderness ratio is shown in Fig. 4, Similarly, the peak strain shows an approximately linear increase with temperature, and the

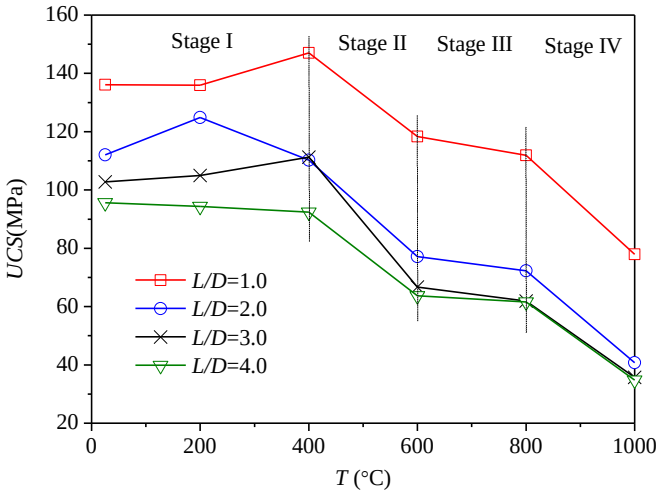

Fig. 5 Evolution of *UCS* with different temperature and slenderness ratio

increasing ratios are 2.16e-5, 1.34e-5, 1.04e-5 and 1.0e-5 per degree centigrade for granite of *L/D*= 1.0, 2.0, 3.0, and 4.0, respectively. The increasing ratio gradually decreases with the increase in slenderness ratio. Thus, the influence of temperature on peak strain is more significant for small slenderness ration specimen.

3.2 Uniaxial compression strength

The uniaxial compression strength (UCS) is one of the most important parameters for geotechnical materials and is widely used for the rock mass classification and stability analysis. With the increase in temperature, the UCS gradually decreases and the evolution law of UCS can be divided into five stages, as shown in Fig. 5. When the temperature is lower than 400ºC, a slight variation of UCS occurs with a maximum increase of 8.04% and a minimum decrease of 3.38% for specimens of *L/D* = 1.0 and 4.0, respectively. When the temperature surpasses 400ºC and locates in the range of 400~600ºC, a significant decrease of 28.70 MPa, 33.13 MPa, 44.54 MPa and 28.70 MPa occurs with respect to slenderness ratios of 1.0, 2.0, 3.0 and 4.0. This is mainly induced by the phase transformation of quartz, from α phase to β phase. And the decreasing amplitude of specimens with small slenderness ratio is larger. When the temperature is in the range of 600~800ºC, the changes in UCS is not apparent with an amplitude of 2.1 MPa~6.48 MPa with a percentage ranging from 3.30~7.21% for the specimens of *L/D*=1.0~4.0. This is induced by the thermal damage cracks, which is induced by solid mineral inflation and fracture of metallic bonding. When the temperature surpasses 800ºC, the UCS significantly decreases and tends to be a constant value for various slenderness ratio specimens, with an average value of 37.10 MPa at *T* = 1000ºC except for the smallest slenderness ratio specimen. This is also induced by the transformation of quartz, from β phase to β-tridymite phase. For the temperatures of *T*=25ºC and 1000ºC, the difference of UCS between specimens of *L/D* = 2.0 and 4.0 decreased from 16.42 MPa to 5.96 MPa. Therefore, the influence of phase transformation on the strength characteristics is significant rather than mineral expansion of high-temperature treated rock samples. On the other hand, the critical slenderness ratio corresponding to the feature mechanical behavior tends to be smaller with the increasing temperature. This is mainly induced by the effects of dehydroxylation and mineral expansion, which induce significant deterioration in strength.

3.3 Microscopic and macroscopic observations

To investigate the influence of temperature on the mineral grains and micro-cracks, the microscopic observation of initially intact samples after various temperatures treated using a scanning electron microscope (SEM) is carried out as shown in Fig. 6. For the indoor temperature granite, mineral grains are closely arrayed, and the spot seems relatively compact and smooth. The intercrystalline crack in Fig. 6(a) is induced by the external force during the sample preparation. When the temperature ranges between 200ºC and 400ºC, a few fissures around the mineral boundaries can be observed, and the fissures are not smooth. A few short transcrystalline cracks can also be found, however the complete cracks throughout minerals have not formed yet. Therefore, the intercrystalline cracks sharply develop due to the differential thermal expansion coefficient of mineralogy. When the temperature reaches 600ºC, obvious transcrystalline cracks and honeycomb defects appear, and those cracks are mainly induced by the transformation of quartz from α phase to β phase. For the granite at 800ºC and 1000ºC, more intercrystalline and transcrystalline cracks appear, and some of the crystal particles have been stripped from the fracture surface, which leads to a rough spot as shown in Fig. 6(e) and 6(f). The stripping defects are mainly induced by the transformation of quartz from β phase to β-tridymite phase. The fracture aperture of intercrystalline crack becomes much larger with the increasing temperature, and the transcrystalline crack becomes more and more obvious when the temperature is higher than 600ºC. The defects induced by chemical effects are much more significant than those of physical changes.

The macroscopic failure patterns of granite with various slenderness ratio and temperature are shown in Fig. 7.

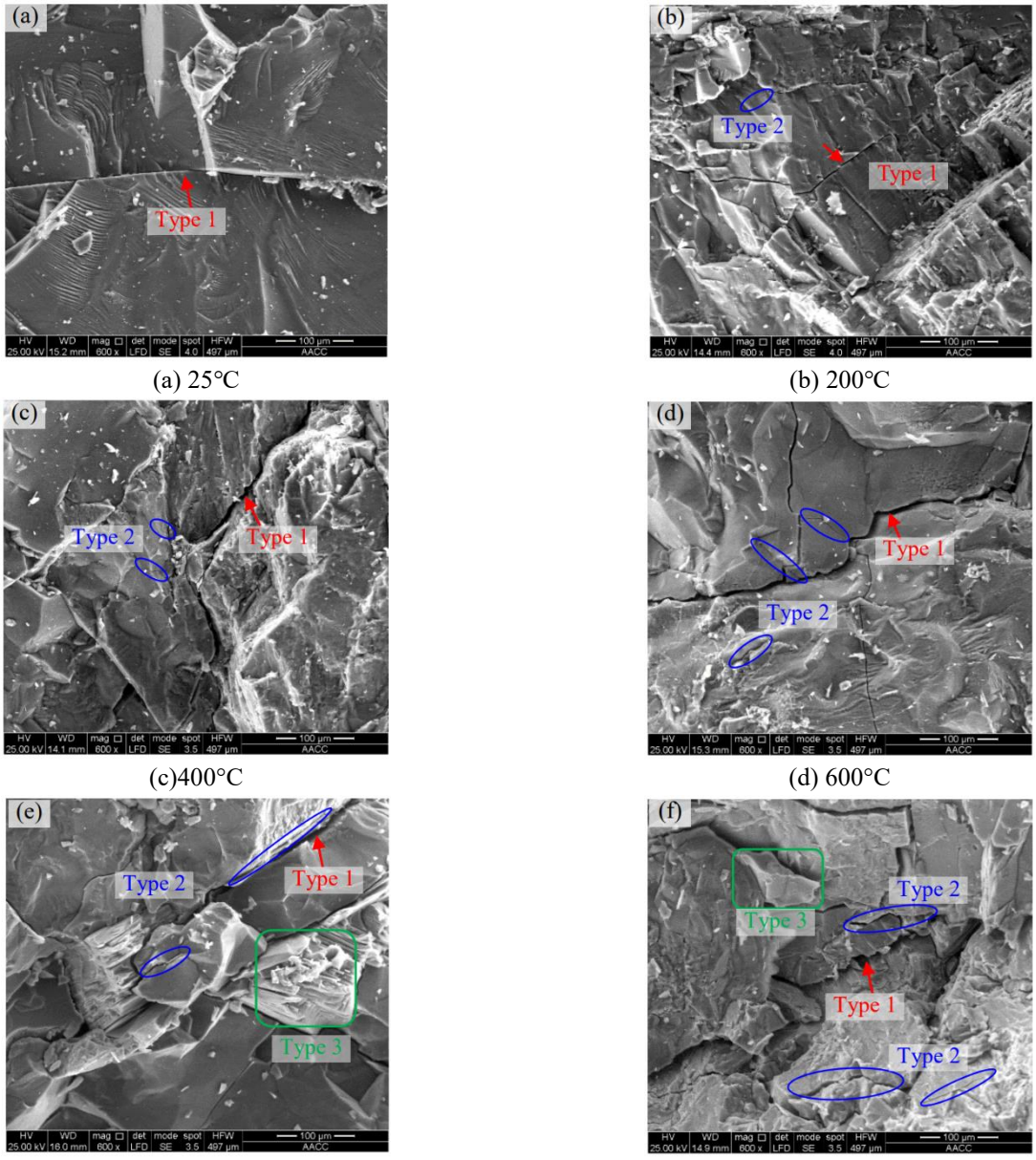

(a) 25℃ (b) 200℃

(c)400℃ (d) 600℃

(e)800℃ (f) 1000℃

Fig. 6 Microscopic observations of granite after high temperature Note: Type 1 denotes the intercrystalline crack; Type 2 denotes the transcrystalline crack; Type 3 denotes the stripping defects

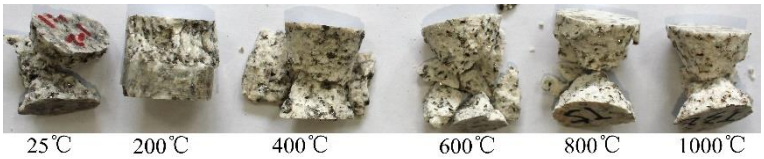

(a) *L*/*D*=1.0

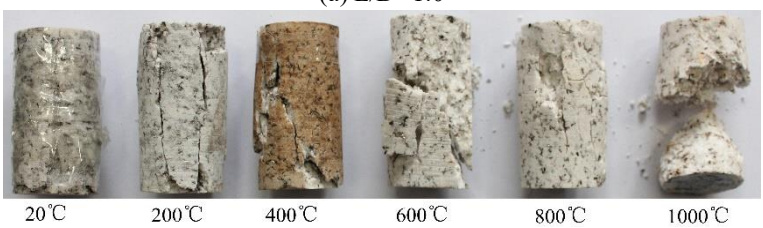

(b) *L*/*D*=2.0

Fig. 7 Macroscopic failure pattern of rock samples

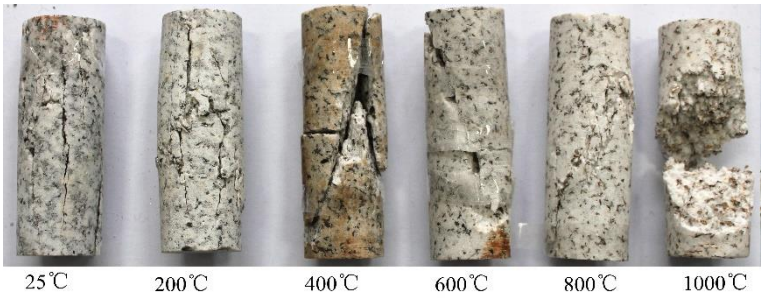

(c) *L*/*D*=3.0

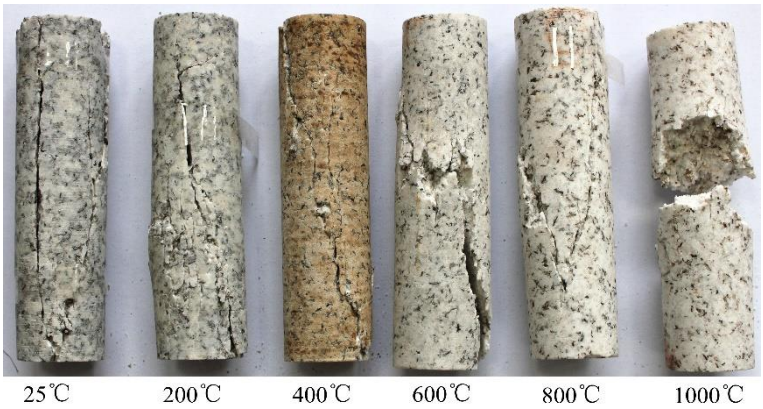

(d) *L*/*D*=4.0

Fig. 7 Continued

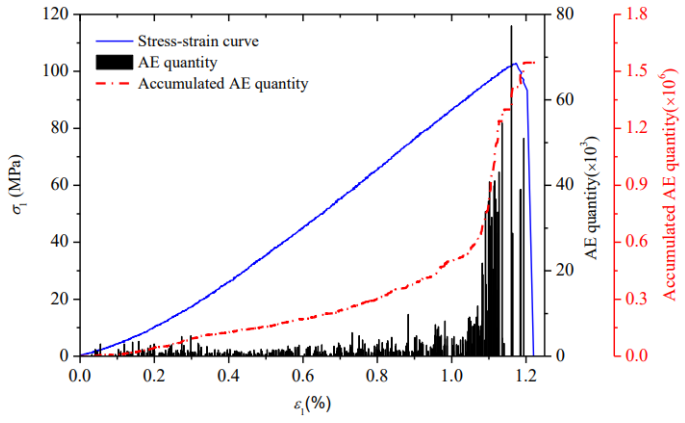

(a) *T*=25°C and *L*/*D*=3.0

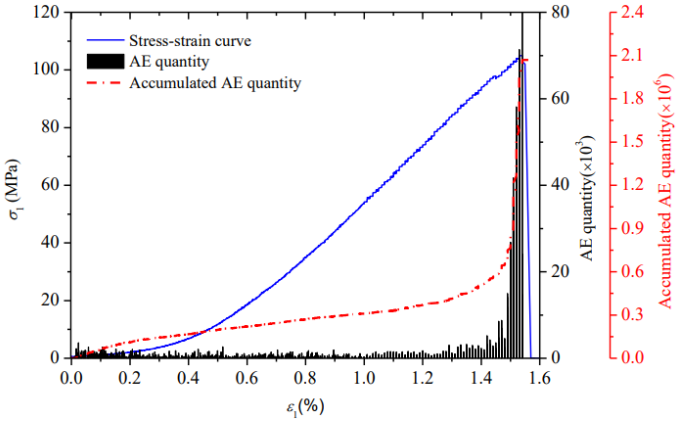

(b) *T*=200°C and *L*/*D*=3.0

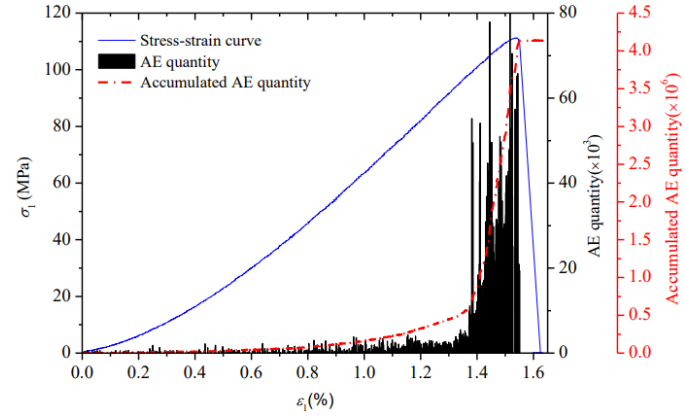

(c) *T*=400°C and *L*/*D*=3.0

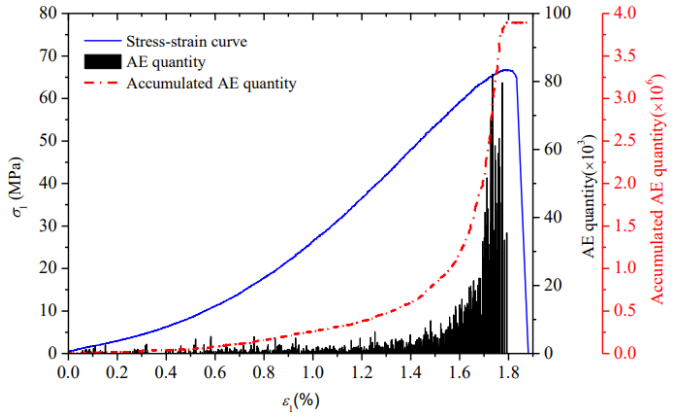

(d) *T*=600°C and *L*/*D*=3.0

Fig. 8 Acoustic emission characteristics of granite with respect to various temperatures and slenderness

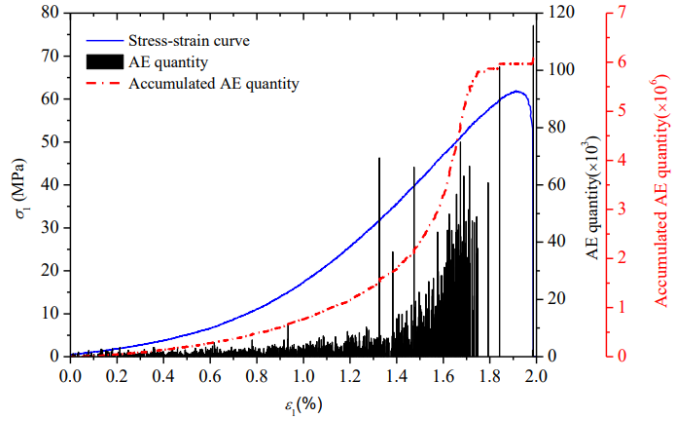

(e) T=800℃ and L/D=3.0,

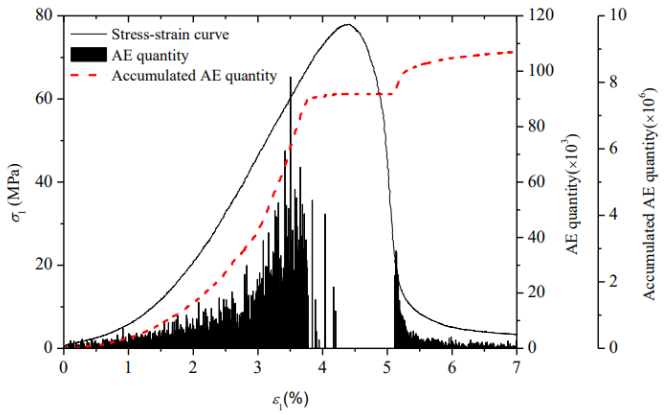

(f) L/D=1.0 and T=1000℃

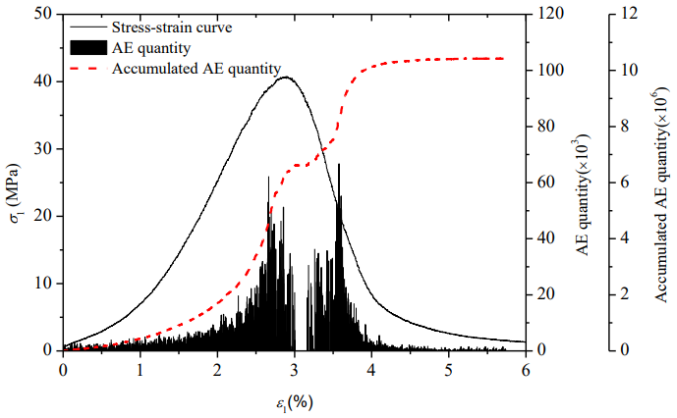

(g) L/D=2.0 and T=1000℃

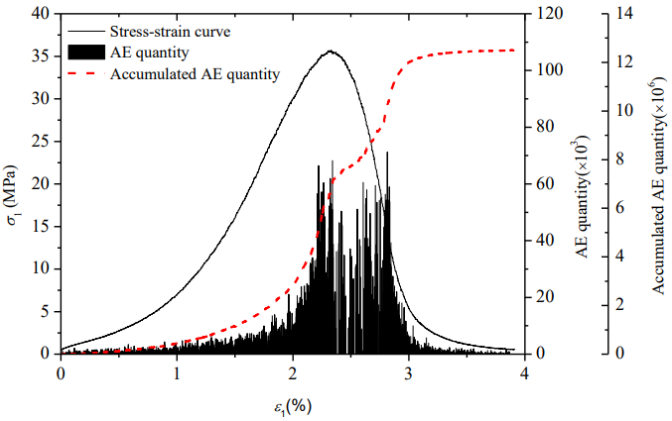

(h) L/D=3.0 and T=1000℃

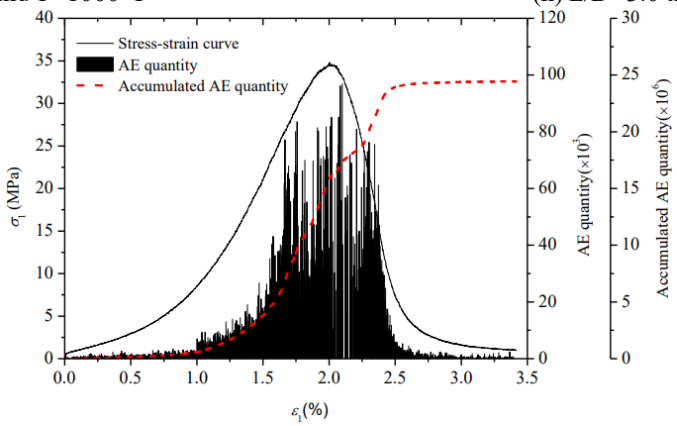

(i) L/D=4.0 and T=1000℃

Fig. 8 Continued

When the slenderness ratio is small, i.e., L/D = 1.0, there are two cones on the two surfaces, which is mainly induced by the friction. The influence of temperature on failure pattern is not obvious, and all of the failures are shear dominant. For the rock samples of L/D = 2.0, tensile failure occurs while T = 200ºC. With the increase in temperature, shear cracks gradually appear, and a tensile dominant tensile-shear mixed failure pattern occurs when T = 400ºC. When the temperature reaches 600ºC, the failure mode turns to be a series of shear dominant cracks, together with a few tensile cracks around the main failure surface. However, once the temperature is higher than 800ºC, both of the axial and circumferential cracks appear, which leads to local ductile failure pattern. When the temperature reaches 1000ºC, the failure region would mainly concentrate upon a small section, which would be damaged as granulate, and an obvious ductile failure pattern would appear. In a word, the circumferential cracks appear at about 600ºC, 600~800ºC, 800ºC and 1000ºC for the specimens of L/D=1.0, 2.0, 3.0 and 4.0. Thus, the critical brittle-ductile transition temperature increases with slenderness ratio.

3.4 Acoustic emission characteristics

The Acoustic emission (AE) characteristics are very

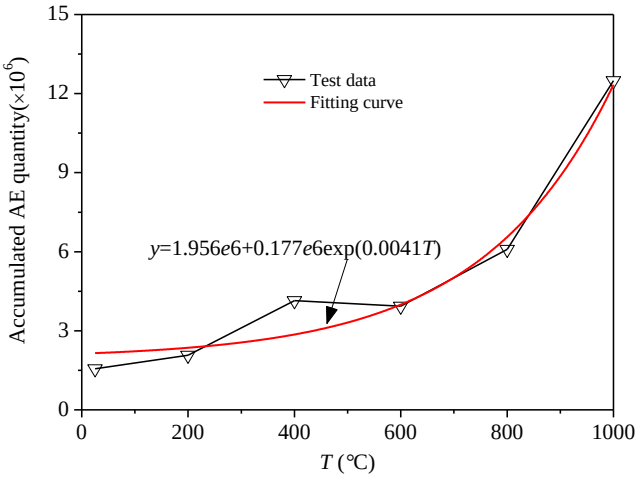

Fig. 9 Accumulated AE quantity of granite with different temperature for *L/D*=3.0

useful for exploring the failure process. Without loss of generality, series of samples with *L/D* = 3 and *T* = 1000ºC are employed to study the influence of temperature and slenderness ratio on the AE characteristics. The AE characteristics of granite specimens with respect to various temperatures and *L/D* = 3.0 are shown in Figs. 8(a)-8(e). The AE characteristics are very similar at *T* = 25~400ºC and can be divided into two typical periods, i.e., a steady period and an active period. In the steady period, the stress-strain curves of granite with various temperatures all show an initial nonlinear behavior with a concave-upward shape, then a linear elastic loading stage occurs. Note that, the AE events are very rare in the steady period due to potential cracks closure. When the axial stress reaches about 70~95% of the peak strength, the AE events significantly increase, and the AE characteristics step into the active period. Once the peak strength is reached, a sudden drop of uniaxial stress happens, which results in a series of larger AE events, and the accumulated AE quantity immediately increases to its maximum value. Moreover, the critical axial strains corresponding to the starting point of active period mainly locates in the range of 1.1~1.5%. Additionally, the influence of slenderness ratio on AE characters is studied according to the series tests with *T*=1000ºC, as shown in Figs. 8(f)-8(i). Before the uniaxial stress approximately reaches the peak strength, the AE characteristics become relatively inactive. And this inactive period decreases for the specimens with respect to large of slenderness ratio. For example, hardly any of AE events happen during the progressive failure process in the post-failure region before residual strength is reached for the specimen of *L/D* = 1.0, however, the relative inactive stage becomes more and more inconspicuous for the specimen of *L/D* = 4.0.

Obviously, The AE events become more and more with increasing temperature as shown in Fig. 9. The accumulated AE quantities for the four kinds of specimens are 8.96e6, 10.42e6, 12.49e6, and 24.44e6, respectively. The AE events increase in a smoother way, which leads to an ambiguous critical starting point corresponding to the active stage. The accumulated AE quantities show an exponent increase with temperature for specimen of *L/D*=3.0, i.e.,

$$N = 1.956 \times 10^6 + 1.77 \times 10^5 \mathrm{e}^{0.0041T} \quad (2)$$

where *N* is the accumulated AE quantities.

4. Conclusions

A series of experimental tests were carried out to study the temperature and slenderness ratio effects on Beishan granite. According to the tests results, major findings can be drawn as follows:

• With the increase in temperature, more and more potential cracks are formed for Beishan granite. When the temperature is lower than 400ºC, the potential damage mainly induces intercrystalline cracks. When the temperature surpasses 600ºC, obvious transcrystalline cracks are formed. The critical brittle-ductile transition temperature increases with slenderness ratio.

• The elastic modulus decreases with temperature, and slightly increases with slenderness ratio. When *T*=1000ºC, the elastic modulus tends to be a constant value of 2.67 GPa. Meanwhile, the peak strain increases with temperature and decreases with slenderness ratio. The influence of temperature on peak strain is more significant for specimens with small slenderness ratio. When the temperature is lower than 400ºC, only a slight change of UCS happens, but a significant decrease occurs when the temperature *T* = 400ºC and 800ºC, which corresponds to the temperature of phase transformation of mineral. The critical slenderness ratio corresponding to the characteristic mechanical behavior tends to be smaller with the increase in temperature.

• The accumulated AE quantity increases with temperature obeying an exponent function, and there exists an inactive period before the peak strength is reached for specimens of *L/D* = 3.0. However, the inactive stage becomes inconspicuous with the increase of slenderness ratio.

Acknowledgments

The authors are grateful to the financial support from the National Natural Science Foundation of China (52074269) and China Postdoctoral Science Foundation (Nos. 2020T130698 and 2018 M640534).

References

Bieniawski, Z.T. (1967), "The effect of specimen size on compressive strength of coal", *Int. J. Rock Mech. Min. Sci.*, **5**(4), 325-335. https://doi.org/10.1016/0148-9062(68)90004-1.

Brotóns, V., Tomás, R., Ivorra, S. and Alarcón, J.C. (2013), "Temperature influence on the physical and mechanical properties of a porous rock: San Julian's calcarenite", *Eng. Geol.*, **167**(4), 117-127. https://doi.org/10.1016/j.enggeo.2013.10.012.

Ding, Q.L, Ju, F., Mao, X.B., Ma, D., Yu, B.Y. and Song, S.B. (2016), "Experimental investigation of the mechanical behavior in unloading conditions of sandstone after high-temperature treatment", *Rock Mech. Rock Eng.*, **49**(7), 2641-2653. https://doi.org/10.1007/s00603-016-0944-x.

Dwivedia, R.D., Goela, R.K., Prasada, V.V.R. and Sinhab, A. (2008), "Thermo-mechanical properties of Indian and other granites", *Int. J. Rock Mech. Min. Sci.*, **45**(3), 303-315. https://doi.org/10.1016/j.ijrmms.2007.05.008.

Ercikdi, B., Karaman, K., Cihangir, F., Yılmaz, T., Aliyazicioglou, S. and Kesimal, A. (2016) "Core size effect on the dry and saturated ultrasonic pulse velocity of limestone samples", *Ultrasonics,* **72**, 143-149. https://doi.org/10.1016/j.ultras.2016.08.006.

Guo, Q.Z., Su, H.J., Liu, J.W., Yin, Q., Jing, H.W. and Yu, L.Y. (2020), "An experimental study on the fracture behaviors of marble specimens subjected to high temperature treatment", *Eng. Fract. Mech.*, **225**, 106862. https://doi.org/10.1016/j.engfracmech.2019.106862.

Jamshidi, A., Zamanian, H. and Sahamieh, R.Z. (2018) "The effect of density and porosity on the correlation between uniaxial compressive strength and P-wave velocity", *Rock Mech. Rock Eng.*, **51**(4), 1-8. https://doi.org/10.1007/s00603-017-1379-8.

Kong, B., Wang, E.Y., Li, Z.H., Wang, X.R., Liu, J. and Li, N. (2016), "Fracture mechanical behavior of sandstone subjected to high-temperature treatment and its acoustic emission characteristics under uniaxial compression conditions", *Rock Mech. Rock Eng.*, **49**(12), 4911-4918. https://doi.org/10.1007/s00603-016-1011-3.

Liu, S. and Xu, J.Y. (2015a), "An experimental study on the physico-mechanical properties of two post-high-temperature rocks", *Eng. Geol.*, **185**, 63-70. https://doi.org/10.1016/j.enggeo.2014.11.013.

Liu, S. and Xu, J.Y. (2015b), "Fractal analysis for dynamic failure characteristics of granite induced by mechanical–thermal loading", *Geotech. Lett.*, **5**(3), 191-197. https://doi.org/10.1680/jgele.15.00035.

Masoumi, H., Saydam, S. and Hagan, P.C. (2016), "Unified size-effect law for intact rock", *Int. J. Geomech.*, **16**(2), 04015059. https://doi.org/10.1061/(ASCE)GM.1943-5622.0000543.

Peng, J., Rong, G., Cai, M., Yao, M.Q. and Zhou, C.B. (2016), "Physical and mechanical behaviors of a thermal-damaged coarse marble under uniaxial compression", *Eng. Geol.*, **200**(12), 88-93. https://doi.org/10.1016/j.enggeo.2015.12.011.

Quiñones, J., Arzúa, J., Alejano, L.R., García-Bastante, F., Mas Ivars, D. and Walton, G. (2017), "Analysis of size effects on the geomechanical parameters of intact granite samples under unconfined conditions", *Acta Geotech.*, **12**(6), 1229-1242. https://doi.org/10.1007/s11440-017-0531-7.

Ranjith, P.G., Daniel, R.V., Bai, J.C., Alarcón, J.C. and Samintha, A.P. (2012), "Transformation plasticity and the effect of temperature on the mechanical behaviour of Hawkesbury sandstone at atmospheric pressure", *Eng. Geol.*, **151**, 120-127. https://doi.org/10.1016/j.enggeo.2012.09.007.

Su, H.J., Guo, Q.Z., Jing, H.W., Yu, L.Y., Liu, J.W. and Gao, Y.N. (2020) "Mechanical performances and pore features of coal subjected to heat treatment in approximately vacuum environment", *Int. J. Geomech.*, **20**(7), 06020011. https://doi.org/10.1061/(ASCE)GM.1943-5622.0001713.

Sun, Q., Zhang, W.Q., Xue, L., Zhang, Z.Z. and Su, T.M. (2015), "Thermal damage pattern and thresholds of granite", *Environ. Earth Sci.*, **74**(3), 2341-2349. https://doi.org/10.1007/s12665-015-4234-9.

Tian, H., Mei, G., Jiang, G.S. and Qin, Y. (2017), "High-temperature influence on mechanical properties of diorite", *Rock Mech. Rock Eng.*, **50**(6), 1661-1666. https://doi.org/10.1007/s00603-017-1185-3.

Wu, J.Y., Feng, M.M., Yu, B.Y. and Han, G.S. (2018), "The length of pre-existing fissures effects on the mechanical properties of cracked red sandstone and strength design in engineering", *Ultrasonics,* **82**, 188-199. https://doi.org/10.1016/j.ultras.2017.08.010.

Yin, T.B., Shu, R.H., Li, X.B., Wang, P. and Liu, X.L. (2016), "Comparison of mechanical properties in high temperature and thermal treatment granite", *Trans. Nonferrous Met. Soc. China*, **26**(7), 1926-1937. https://doi.org/10.1016/S1003-6326(16)64311-X.

Zhang, L.Y., Mao, X.B., Liu, R.X., Guo, X.Q. and Ma, D. (2014), "The mechanical properties of mudstone at high temperatures: An experimental study", *Rock Mech. Rock Eng.*, **47**(4), 1479-1484. https://doi.org/10.1007/s00603-013-0435-2.

Zhang, X.P., Zhang, Q. and Wu, S.C. (2017), "Acoustic emission characteristics of the rock-like material containing a single flaw under different compressive loading rates", *Comput. Geotech.*, **83**, 83-97. https://doi.org/10.1016/j.compgeo.2016.11.003.

IC